Water Research X 25 (2024) 100260

Contents lists available at ScienceDirect

Water Research X

journal homepage: www.sciencedirect.com/journal/water-research-x

An overlooked nanofluids effect from Fe_3O_4 nanoparticles enhances mass transfer in anammox granular sludge

Dongdong Xu [a,b], Aqiang Ding [c], Yang Yu [a], Ping Zheng [a], Meng Zhang [a], Zhetai Hu [b,*]

[a] Department of Environmental Engineering, College of Environmental & Resource Sciences, Zhejiang University, Hangzhou, China
[b] Australian Centre for Water and Environmental Biotechnology (ACWEB, formerly AWMC), The University of Queensland, St. Lucia 4072, Queensland, Australia
[c] Department of Environmental Science, College of Environment and Ecology, Chongqing University, Chongqing 400045, China

ARTICLE INFO

Keywords:
Anammox granular sludge
Fe3O4 nanoparticles
Fe3O4 microparticles
Nanofluids effect
Synthesis of key enzymes
Substrate accessibility

ABSTRACT

Magnetite (Fe_3O_4) particles have been widely reported to enhance the anammox's activity in anammox granular sludge (AnGS), yet the underlying mechanisms remain unclear. This study demonstrates that both Fe_3O_4 microparticles (MPs) and nanoparticles (NPs) at a dosage of 200 mg Fe_3O_4/L significantly increased the specific anammox activity (SAA) of AnGS. Additionally, the transcriptional activities of the *hzs* and *hdh* genes involved in the anammox process, as well as the heme *c* content in AnGS, were also notably enhanced. Notably, Fe_3O_4 NPs were more effective than MPs in boosting anammox activity within AnGS. Mechanistically, Fe_3O_4 MPs released free iron, which anammox bacteria utilized to promote the synthesis of key enzymes, thereby enhancing their activity. Compared to MPs, Fe_3O_4 NPs not only elevated the synthesis of these key enzymes to a higher level but also induced a nanofluids effect on the surface of AnGS, improving substrate permeability and accessibility to intragranular anammox bacteria. Moreover, the nanofluids effect was identified as the primary mechanism through which Fe_3O_4 NPs enhanced anammox activity within AnGS. These findings provide new insights into the effects of nanoparticles on granular sludge systems, extending beyond AnGS.

1. Introduction

Anammox has been recognized as a highly promising biological nitrogen remove process due to its high efficiency, cost-effectiveness, and low carbon footprint (Kartal et al., 2010; Zheng et al., 2024). Although the anammox-based nitrogen removal process has been adopted globally, its stable and efficient operation is often hindered by the slow growth rate of anammox bacteria (Strous et al., 1999; Lotti et al., 2015), and their low adaptability to changing environmental conditions (van der Star et al., 2007; Jin et al., 2012; Su et al., 2023). Anammox granular sludge (AnGS), which serves as a habitat for anammox bacteria, can harbor sufficient biomass and has strong capacity to resist various stresses such as antibiotics and heavy metals (Hou et al., 2015; Tang et al., 2017; Wang et al., 2023). Despite its significant application potential, the poor activity of anammox bacteria in AnGS is often reported, potentially attributed to the lack of essential materials (e.g. iron) for the synthesis of key metabolic enzymes, and the inefficient substrate transfer from the exterior to interior of granule (Shi et al., 2017; Xu et al., 2021a; Dong et al., 2023). Overall, enhancing anammox activity in AnGS is vital to further expand the application of this sustainable nitrogen removal process.

Some studies have demonstrated Fe_3O_4 nanoparticles (NPs) dosage significantly increases the specific anammox activity (SAA) in AnGS (Xu et al., 2020; Chen et al., 2021). For instance, Chen et al. (2021) conducted batch tests and found that adding Fe_3O_4 NPs at 100 mg Fe_3O_4/L increased SAA from ~312 to ~423 mg-N/g-VSS/d. Similarly, a long-term test by Xu et al. (2020) observed a significant increase in SAA from 287.0 ± 13.0 to 381.8 ± 15.7 mg-N/g-VSS/d with the addition of Fe_3O_4 NPs at 200 mg Fe_3O_4/L. Also, the introduction of Fe_3O_4 NPs at 200 mg/L led to an increase in heme *c* content from 1.6 to 2.7 μmol/g VSS, and the anammox bacterial (*Candidatus* Kuenenia) abundance from 25.1% to 33.4%. Despite numerous reports indicating the SAA enhancement by adding Fe_3O_4 NPs, the underlying mechanism remains poorly understood (Dai et al., 2023). Some researchers have suggested a potential mechanism whereby Fe_3O_4 NPs attaches to the AnGS surface and subsequently releases free iron ions (Fe^{2+} or Fe^{3+}), which can be utilized by anammox bacteria for synthesizing key metabolic enzymes (Weng et al., 2023). However, this hypothesis has yet to be clearly confirmed.

It is widely reported that the addition of NPs induces a nanofluids

* Corresponding author.
E-mail address: Zhetai.hu@uq.edu.au (Z. Hu).

https://doi.org/10.1016/j.wroa.2024.100260
Received 29 August 2024; Received in revised form 19 September 2024; Accepted 25 September 2024
Available online 26 September 2024

effect that can significantly enhance water permeability in capillary pores, thereby improving mass transfer efficiency (Yu et al., 2015; Li et al., 2019; Fu et al., 2021). For instance, Fu et al. (2021) reported that dosing Fe_3O_4 NPs at a volume concentration between 0.00125% and 0.01% improved the capillary permeability of pore channels by 8–75%. Indeed, the surface of AnGS is filled with capillary pores (Xu et al., 2021a). When NPs attach to its surface, they may induce a nanofluids effect, enhancing the transfer efficiency of substrates (e.g. ammonium and nitrite) to the interior anammox bacteria within AnGS. As a common phenomenon associated with the addition of NPs, the nanofluids effect could play a crucial role in enhancing SAA in an NPs-added AnGS process. However, this phenomenon also has not been experimentally revealed.

Therefore, it is possible that the Fe_3O_4 NPs addition increases the SAA in AnGS through two different pathways: 1) Releasing the free iron ions for anammox bacteria to synthesize key metabolic enzymes; 2) enhancing substrate transfer efficiency via nanofluids effect. This study aims to systematically investigate the effects of Fe_3O_4 NPs on AnGS, focusing on these two pathways. To this end, AnGS was sourced from a culture bioreactor and exposed to Fe_3O_4 particles at different particle sizes (~50 nm and ~60 μm) and concentrations (50–500 mg Fe_3O_4/L). First, SAA and transcription level of key metabolic enzymes were tested under various Fe_3O_4 particles exposure conditions to assess their impact on overall anammox bacterial activity. Subsequently, intracellular iron contents were determined to examine the effects of Fe_3O_4 particles on bacterial iron absorption. Finally, the substrate accessibility of anammox bacteria was analyzed to evaluate the impacts of Fe_3O_4 particles on granular mass transfer.

2. Results

2.1. The effects of Fe_3O_4 particles on the SAA of AnGS

Fig. 1 presents the impact of Fe_3O_4 particles of varying sizes (NPs and MPs) and concentrations on the SAA of AnGS. The initial SAA of AnGS was 394.8 ± 18.4 mg-N/g-VSS/d, a value comparable to that reported in the literature (Xu et al., 2021b). Clearly, Fe_3O_4 particles addition changed the granular SAA. Specifically, exposure to Fe_3O_4 NPs at 50, 100, and 200 mg Fe_3O_4/L promoted SAA to 423.8 ± 15.3, 461.7 ± 14.2, and 570.1 ± 16.0 mg-N/g-VSS/d, respectively, showing average increases of ~7.5% ($p > 0.05$), ~17.1% ($p < 0.05$), and ~44.6% ($p < 0.05$), compared to the initial SAA (Fig. 1a). However, when the dosage of Fe_3O_4 NPs further increased to 500 mg Fe_3O_4/L, the SAA reduced by ~13.9% ($p < 0.05$), reaching 339.8 ± 13.4 mg-N/g-VSS/d. Fe_3O_4 MPs exhibited the similar trend while with weaker effects on SAA. Notably, with the rose of Fe_3O_4 dosage, the difference in SAA between NPs and MPs groups widened, suggesting that Fe_3O_4 NPs had more significant impact on anammox bacteria in AnGS than that of Fe_3O_4 MPs.

The ratios of removed nitrite to removed ammonium, and produced nitrate to removed ammonium were 1.38±0.13 and 0.24±0.03, respectively, in the control (Fig. 1b). These values in NPs-dosed groups and MPs-dosed groups were similar ($p > 0.05$) and close to theoretical values of anammox reaction stoichiometry, with ratios of 1.32 and 0.26, suggesting the nitrogen was mainly removed by anammox bacteria in these tests.

2.2. The effects of Fe_3O_4 particles on the metabolic activity of anammox bacteria within AnGS

Meta-transcriptomics analysis was conducted to further explore effects of Fe_3O_4 particles on the anammox bacterial metabolic activity in AnGS. *Candidatus* Kuenenia, which was the sole detected anammox bacterial genus, showed the highest expression activity (Fig. S1). Hydrazine synthase (*hzs*) and hydrazine dehydrogenase (*hdh*) are critical enzymes in the metabolic pathway of anammox bacteria (Feng et al., 2023). Fig. 2a&b illustrates the impact of Fe_3O_4 particles at a dosage of 200 mg Fe_3O_4/L on the transcriptional activity of *hzs* and *hdh* genes. Following a 2 h exposure to Fe_3O_4 NPs, the transcriptional activity of *hzs* and *hdh* genes rose by ~111.7% and ~60.9%, respectively, compared with the control, implying Fe_3O_4 NPs significantly enhanced the anammox bacterial metabolic activity of anammox bacteria ($p < 0.05$). On the other hand, Fe_3O_4 MPs dosing notably ($p < 0.05$) increased the transcriptional activity of *hzs* gene (~30.7%), while its impact on *hdh* gene was insignificant ($p > 0.05$). After exposure for 4 h, the transcription levels of *hzs* and *hdh* genes declined in all three groups, which primarily attributed to substrate consumption during the batch test (Fig. S2) (Wang et al., 2016). Nonetheless, the differences in transcriptional activity of *hzs* and *hdh* genes among three groups remained similar with those observed at 2 h (Fig. 2). Overall, Fe_3O_4 NPs had a stronger promoting effect on metabolic activity of anammox bacteria compared to Fe_3O_4 MPs, consistent with the SAA tests.

Cytochrome *c*, indicative of anammox bacterial activity, is reflected by heme *c* content (Ma et al., 2019; Kang et al., 2020). Heme *c* contents in the Fe_3O_4 NPs-dosed group were ~16.0% and ~18.4% higher than those in control at 2 and 4 h, respectively ($p < 0.05$) (Fig. 2c). While the Fe_3O_4 MPs-dosed group showed the same trend but to lower degrees.

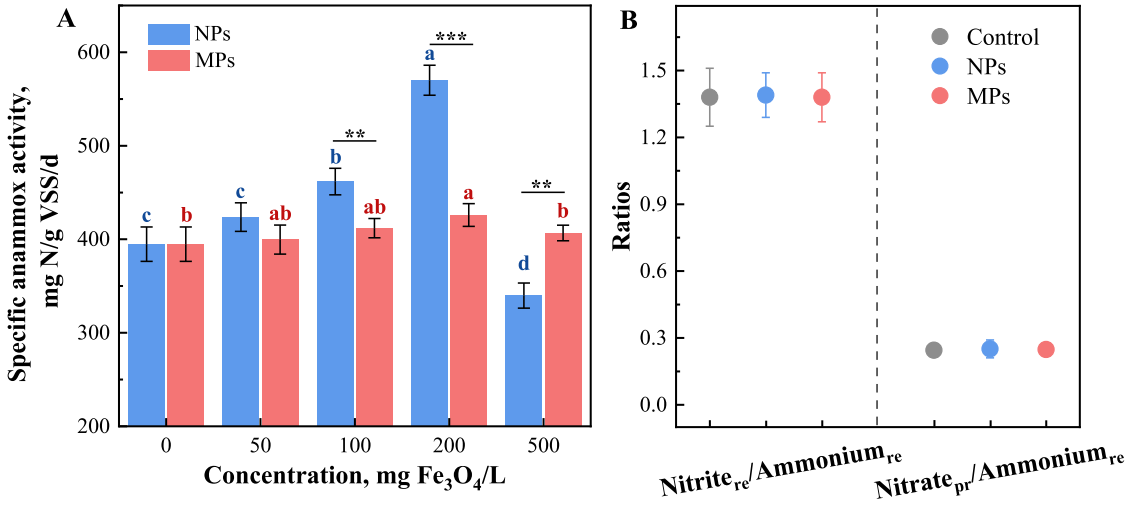

Fig. 1. The SAA of AnGS under different Fe_3O_4 particles exposure conditions (A); The ratios between removed nitrite and ammonium, and between produced nitrate and removed ammonium during the SAA tests (B). $Nitrite_{re}$, $Ammonium_{re}$, and $Nitrate_{pr}$ in Fig. 1B refer to the removed nitrite, removed ammonium, and produced nitrate, respectively. ** and *** refer to $p < 0.01$ and $p < 0.001$, respectively.

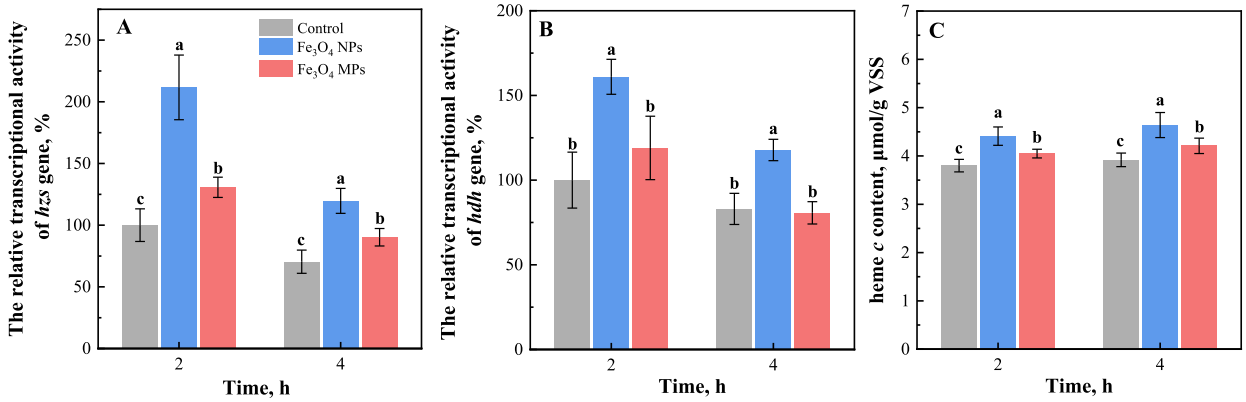

Fig. 2. Transcriptional activity of *hzs* (A) and *hdh* (B) gene of anammox bacteria and the heme *c* content of AnGS (C) in the control, NPs-dosed (200 mg Fe_3O_4/L), and MPs-dosed (200 mg Fe_3O_4/L) groups during a run of batch tests. The data of Fig. 2A&B were all normalized based on obtained values in the control group at 2 h.

Iron-sulfur proteins, which play vital roles in the electron transport of anammox bacteria, are also highly correlated with bacterial activity (Feng et al., 2023). Compared with the control group, transcription levels of most genes related to iron-sulfur protein synthesis in NPs-dosed group were up-regulated by 15.2–31.6% at 2 h, which further slightly increased at 4 h. MPs-dosed group exhibited a similar trend but the smaller range (Fig. S3). These results supported the superior activity of anammox bacteria receiving Fe_3O_4 NPs.

2.3. The impacts of Fe_3O_4 particles on the intracellular iron content

Fe_3O_4 particles releases iron ions that anammox bacteria utilize for synthesizing key metabolic enzymes (Weng et al., 2023). The Fe_3O_4 NPs dosage (200 mg Fe_3O_4/L) increased the transcriptional activity of the ferrous iron transport protein-related gene by ~5.9% ($p > 0.05$) at 2 h and ~21.4% ($p < 0.05$) at 4 h, compared with the control (Fig. 3a). Similarly, Fe_3O_4 NPs significantly ($p < 0.05$) elevated the transcriptional activity of the ferrous uptake regulator protein-related gene by ~18.7% and ~23.1% at 2 and 4 h, respectively (Fig. 3b). Consequently, intracellular iron content significantly rose by ~14.2% and ~21.1% at the corresponding time points, respectively ($p < 0.05$) (Fig. 3c), implying that anammox bacteria indeed uptake and utilized the free iron ions released from Fe_3O_4 NPs. Interestingly, the effects of NPs and MPs on these indicators were similar, contrasting with results of SAA and metabolic activity tests, suggesting that, apart from enhancing bacterial iron absorption to synthesize key metabolic enzymes, Fe_3O_4 NPs should play an additional role in increasing the activity of anammox bacteria within AnGS.

2.4. The impacts of Fe_3O_4 particles on substrate transfer efficacy within AnGS

2.4.1. Substrate accessibility of anammox bacteria

We hypothesized that the presence of Fe_3O_4 NPs would enhance the accessibility of substrates for anammox bacteria within AnGS. The effects of Fe_3O_4 particles (200 mg Fe_3O_4/L) on ammonium and nitrite concentrations in the medium and within cells were investigated (Fig. 4). To mitigate substrate limitations, ample amounts of initial ammonium and nitrite were added, resulting in concentrations of 35–45 and 35–55 mg-N/L, respectively, in the medium. Following exposure to Fe_3O_4 NPs for 20 mins, the intracellular concentrations of ammonium and nitrite increased to ~5.2 and ~0.89 mg-N/L, respectively, both significantly higher than the corresponding values (~3.9 and ~0.72 mg-N/L) in the control ($p < 0.05$). However, extending the exposure duration to 40 mins did not further elevate the intracellular concentrations of ammonium and nitrite. On the other hand, AnGS treated with Fe_3O_4 MPs showed similar intracellular ammonium and nitrite concentrations to the control, indicating MPs were ineffective in enhancing substrate accessibility for anammox bacteria within AnGS.

2.4.2. Mass transfer performance of AnGS

To gain insight into the effects of Fe_3O_4 particles on substrate transfer, the spatial distribution of fluorescent microbeads in AnGS under Fe_3O_4 particle exposure (200 mg Fe_3O_4/L) was tested. At a

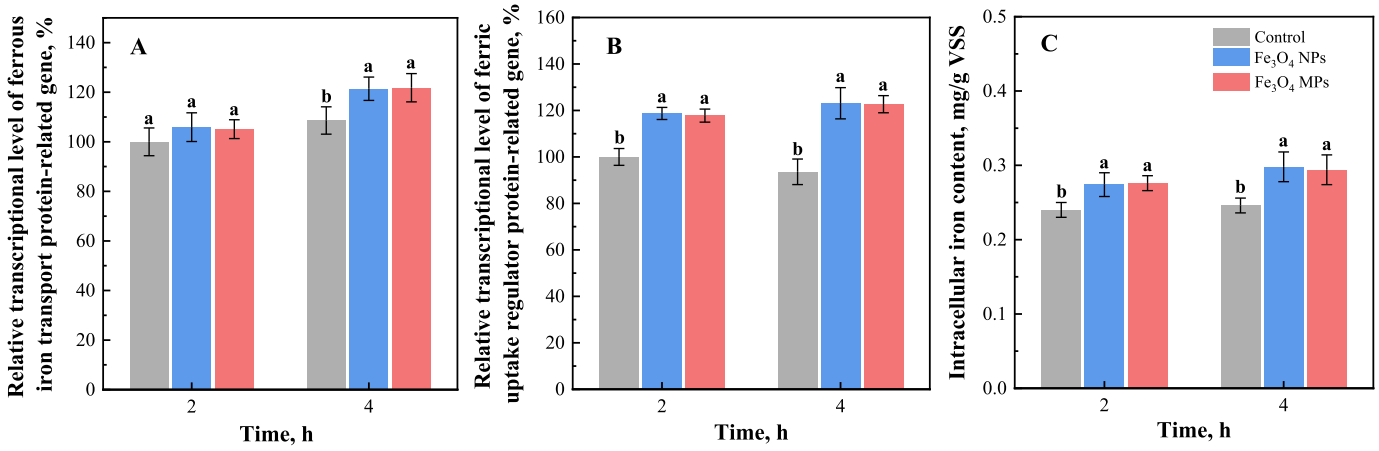

Fig. 3. Transcriptional level of iron transport protein-related genes (A, B) and intracellular iron content (C) in the control, NPs-dosed (200 mg Fe_3O_4/L), and MPs-dosed (200 mg Fe_3O_4/L) groups during a run of batch tests. The data of transcriptional level were all normalized based on obtained values in the control group at 2 h.

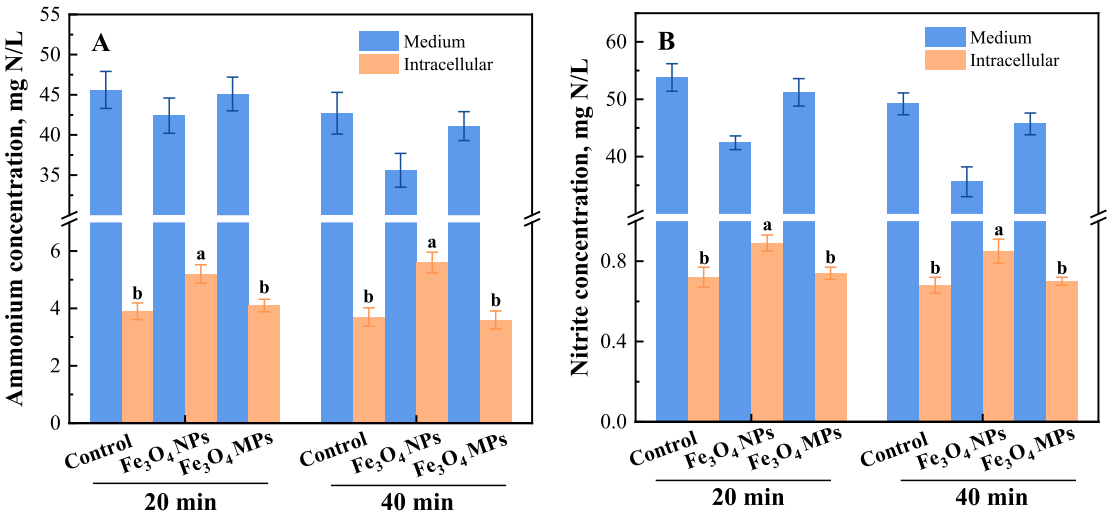

Fig. 4. The impacts of Fe_3O_4 particles (200 mg Fe_3O_4/L) on the concentrations of ammonium (A) and nitrite (B) in the medium and cell after exposure for 20 and 40 mins, respectively.

consistent dosage of fluorescent microbeads, a higher concentration within AnGS indicates better permeability. After 5 mins of cultivation, more microbeads were observed on the surface and interior of NPs-treated AnGS compared to control and MPs-treated AnGS (Fig. 5&S4). The microbeads intensity in the NPs-treated AnGS was quantified to be more than twice as high as in the other two groups, demonstrating that Fe_3O_4 NPs notably enhanced mass transfer permeation in AnGS.

The granular permeability was further assessed by measuring the Γ value through settling experiments. A higher Γ value indicates better granular permeability (Mu et al., 2006). The Γ value for NPs-treated AnGS was significantly higher than those of control and MPs-treated AnGS ($p < 0.05$) (Fig. S5), confirming the improved granule permeability and substrate accessibility for anammox bacteria.

3. Discussion

3.1. Potential mechanism of the AnGS activity enhancement by Fe_3O_4 particles

This study investigates two potential pathways through which Fe_3O_4 particles enhance AnGS's activity: enhancing key metabolic enzymes synthesis and improving substrate accessibility.

Both MPs and NPs increased the SAA of AnGS (Fig. 1). Also, this study observed a significant increase in the transcriptional activity of two key enzymes of anammox bacteria, *hzs* and *hdh*, in AnGS treated with Fe_3O_4 particles (Fig. 2a&b). This is attributed to Fe_3O_4 particles releasing free iron, which could be absorbed by anammox bacteria and utilized for synthesizing key metabolic enzymes (Wang et al., 2022). This study observed an increase in heme *c* content and transcriptional levels of iron-sulfur protein-related genes in AnGS after Fe_3O_4 particle addition (Fig. 2C&S3). Indeed, anammox bacteria rely heavily on

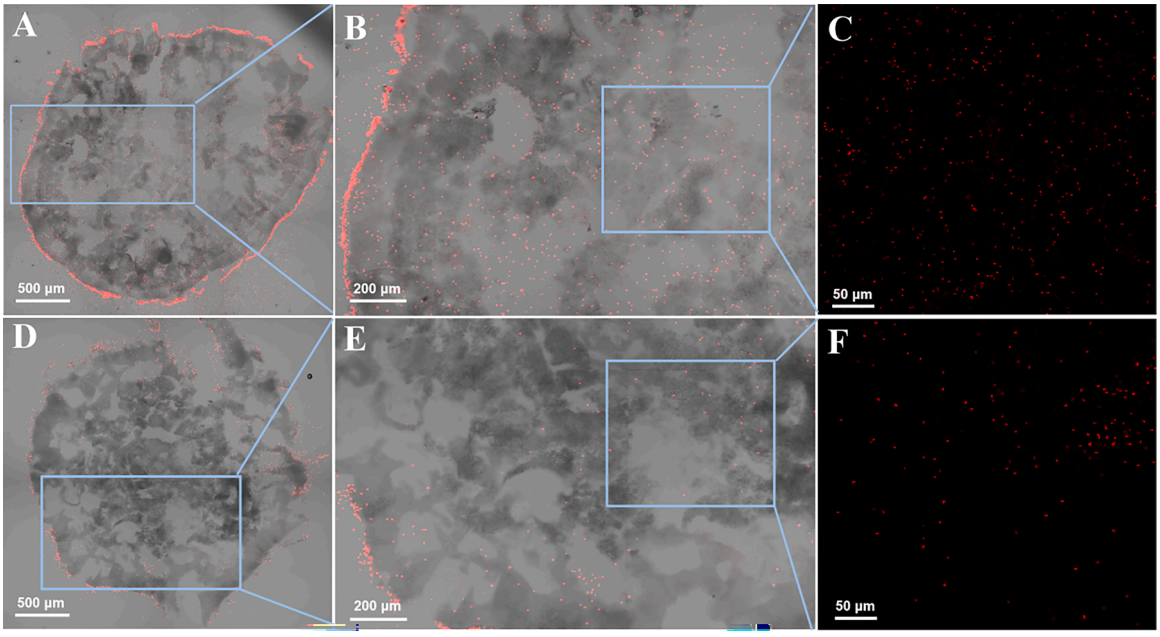

Fig. 5. Distribution of fluorescent microbeads in sections of AnGS. A-C: NPs-dosed (200 mg Fe_3O_4/L); D-F: the control group. The size of fluorescent microbeads was ~1 μm.

iron-containing cofactors like heme *c*, iron-sulfur clusters, and iron-nickel proteins within their anammoxosome (Ferousi et al., 2017). The released iron was used by anammox bacteria, increasing the intracellular iron content (Fig. 3), thereby enhancing their metabolic activity and the performance of AnGS. However, AnGS treated with NPs and MPs showed similar intracellular iron content while different SAAs. Thus, the explanation of additional free iron only partially accounts for the effects of Fe_3O_4 NPs.

This study, for the first time, proposed another potential mechanism of enhancing the performance of AnGS by Fe_3O_4 NPs, i.e. increasing the substrate accessibility. The Fe_3O_4 NPs-dosed AnGS had higher transcriptional activities in most genes related to ammonium and nitrite transporter, compared to those of MPs-dosed and control groups (Fig. S6). Also, the AnGS receiving Fe_3O_4 NPs had significantly higher intracellular ammonium and nitrite concentrations than the other two groups (Fig. 4). These results suggested that Fe_3O_4 NPs addition markedly increased the anammox bacterial substrate obtain rate (Bagchi et al., 2016). Moreover, fluorescent microbeads tracer and settling experiments tests together showed that NPs enhanced the substrate permeability of AnGS, increasing substrate accessibility for intragranular anammox bacteria.

Indeed, the pore sizes investigated in this study ranged from 1 to 50 μm in the surface layer of AnGS. These small pores exhibit high capillary resistance, leading to poor substrate permeability and insufficient accessibility for inner anammox bacteria (Xu et al., 2021a). Fe_3O_4 particles at ~50 nm could penetrate these granular pores and migrate to the solid-liquid interface (Fig. S7). The strong Brownian motion of NPs at this interface could reduce friction resistance between water and pores, promoting the boundary slip and enhancing water permeability-a typical nanofluids effect (Yu et al., 2015; Fu et al., 2021). This effect could reduce capillary resistance in the surface layer of AnGS, facilitating substrate permeability and accelerating ammonium and nitrite transfer rates into granular interior, enhancing the metabolic activity of anammox bacteria within AnGS (Fig. 6).

Overall, Fe_3O_4 NPs induced significantly greater SAA and metabolic activity increments than Fe_3O_4 MPs, despite similar intracellular iron content. Thus, the nanofluids effect induced by Fe_3O_4 NPs was likely the primary reason for enhancing AnGS performance.

3.2. Significance of this work

Anammox bacteria have been widely used for removing nitrogen from various wastewater sources. To enhance their adaptation to diverse engineering environments, enriching anammox bacteria in granule (i.e. AnGS) is frequently recommended (Tang et al., 2011). However, the AnGS activity is often limited due to the lack of essential materials (e.g. iron) for the synthesis of key metabolic enzymes, and the inefficient substrate transfer (Xu et al., 2021a; Dong et al., 2023). This study first elucidated how Fe_3O_4 NPs enhance performance of AnGS, revealing that they enhance the synthesis of key enzymes and induce a nanofluids effect, with the latter being primary reason for SAA enhancement. The discovery of nanofluids effect in this study opens new avenues for understanding impacts of NPs on granular systems, beyond just AnGS. Moreover, the effects of Fe_3O_4 NPs on anammox sludge bed reactor will be further investigated. The obtained optimal dosage and frequency can be applied to guide the promotion of the nitrogen removal performance of anammox reactors.

If Fe_3O_4 NPs can induce a nanofluids effect, it raises the question of whether other NPs can have similar effects. However, many studies have reported adverse effects of some NPs on AnGS (e.g., silver, CuO, and ZnO) (Zhang et al., 2017b; Peng et al., 2019; Zhao et al., 2019). For instance, Zhao et al. (2019) observed a reduction in anammox activity by 18.4%, 35.5%, and 50.4% when exposed to ZnO NPs for 24 h at concentrations of 5, 50, and 150 mg ZnO/L, respectively. Both dosed NPs and released zinc cations can penetrate into granules, increasing reactive oxygen species and thereby reducing the viability of anammox bacteria. In contrast to the release of toxic heavy metals (e.g. Zn^{2+} and Cu^{2+}) from some NPs, Fe_3O_4 NPs release Fe^{2+} and Fe^{3+}, which are heavily required by anammox bacteria for synthesizing essential iron-containing cofactors (Ferousi et al., 2017). Thus, we hypothesize that while dose of other NPs may also induce nanofluids effect, bringing more substrate to intergranular anammox bacteria, the synchronous penetration of toxic heavy metals into granules could prove lethal for the anammox bacteria. However, future studies are needed to confirm this

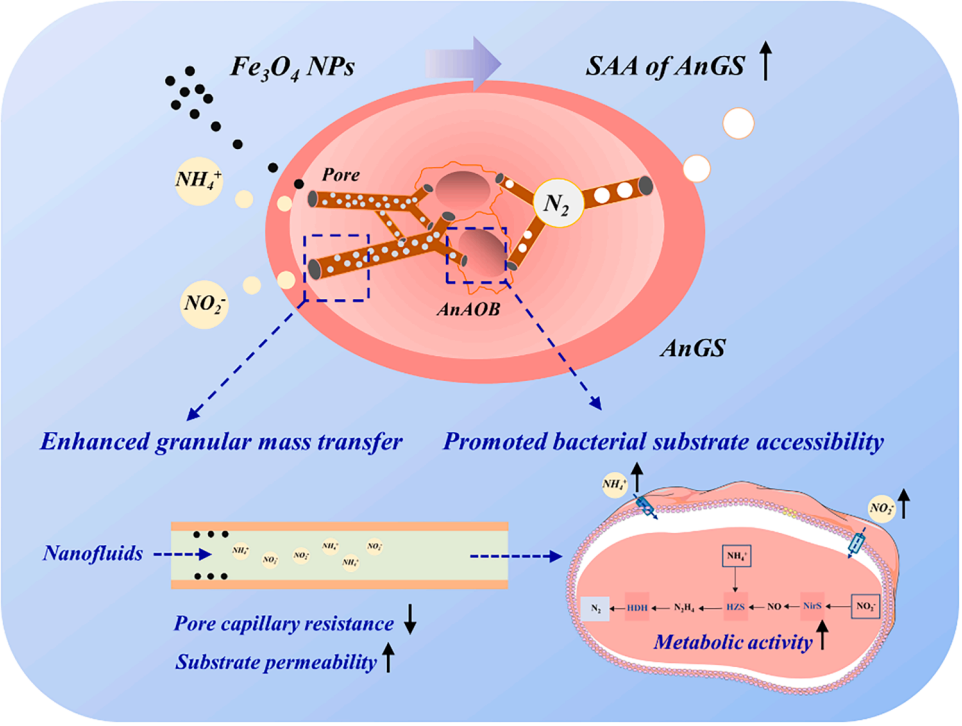

Fig. 6. Potential mechanism for enhancement of substrate transfer efficiency by nanofluids effect. AnAOB refer to anammox bacteria.

hypothesis.

4. Conclusions

In this study, the effects of Fe_3O_4 particles on the performance of AnGS were comprehensively investigated and the underlying mechanism was revealed. The major conclusions include:

1) Dosing Fe_3O_4 NPs and MPs with 200 mg Fe_3O_4/L both significantly increased the SAA of AnGS, while the former exhibited the stronger effectiveness in enhancing anammox activity within AnGS.
2) Both Fe_3O_4 NPs and MPs could release the free iron, which was then utilized by anammox bacteria to promote the synthesis of key metabolic enzymes, thereby increasing their activity.
3) The induced nanofluids effects of Fe_3O_4 NPs improved substrate permeability and increased substrate accessibility to intragranular anammox bacteria, which was identified as the primary mechanism through which Fe_3O_4 NPs enhanced anammox activity within AnGS.

Overall, these findings open the new avenue for understanding the impacts of nanoparticles on granular sludge systems, extending beyond AnGS alone.

5. Materials and methods

5.1. Anammox granular sludge and Fe_3O_4 particles

The AnGS used in this study was collected from a long-term operated lab-scale expanded granule sludge bed (EGSB) reactor (Figure S8A), which was operated for over two years with a stable nitrogen loading rate (NLR) and nitrogen removal rate (NRR) of ~9.9 and ~8.9 kg-N/m^3/d, respectively. The concentrations of volatile suspended solids (VSS) and the ratio of VSS to total suspended solids (TSS) of the enriched AnGS were ~16.9 g/L and ~0.86, respectively. According to previous study (Xu et al., 2021a), the granular mass transfer was weakened with the increase of size. Specifically, when size of AnGS exceeds 2.0 mm, its permeability almost disappeared due to the denser surface layer and smaller pore sizes. Thus, to highlight the effect of Fe_3O_4 particles on granular mass transfer capacity, AnGS with the size over 2.0 mm (accounted for the proportion of over 65% in volume) was selected for the following tests (Figure S8B).

Fe_3O_4 particles with purity of 99.5% were purchased from Aladdin Reagent (Shanghai, China). The size of Fe_3O_4 NPs and microparticles (MPs) was ~50 nm and ~60 μm, respectively. To avoid the aggregation of Fe_3O_4 particles, the stock solution, with a concentration of 2.0 g Fe_3O_4/L, was prepared following the methods reported in literature (Xu et al., 2020).

5.2. Determinations of SAA under different exposure of Fe_3O_4 particles

Batch tests, in triplicate, were performed to investigate the effects of different concentrations (50, 100, 200, and 500 mg Fe_3O_4/L) of Fe_3O_4 NPs and MPs on SAA of AnGS. For each batch test, about 8.0 g wet AnGS was collected and washed with 0.1 M phosphate buffer solution three times. After that, the clean AnGS was added to a 500 mL serum bottle, along with the medium solution (Table. S1). Subsequently, a certain amount of Fe_3O_4 particles stock solutions (2.0 g Fe_3O_4/L) were dosed into the serum bottles to increase the Fe_3O_4 concentration to the predesigned levels. Afterwards, the serum system was sparged with a mixed gas of CO_2 and argon for 20 mins to remove the oxygen within the system. Following this, 1.0 mL ammonium stock solution ($(NH_4)_2SO_4$ of 20.0 g-N/L) and 1.0 mL of nitrite stock solution ($NaNO_2$ of 24.0 g-N/L) were added to the bottle to elevate the initial ammonium and nitrite concentrations to ~50 and ~60 mg-N/L, respectively. The batch reactors were mixed by a sharker at a speed of 180 rpm. The tests were performed at a temperature of about 35 °C. Each test lasted for 6 h, during which 1.0 mL mixed liquid were collected hourly for the determination of concentrations of ammonium, nitrite, and nitrate. The SAA was determined as the volumetric total nitrogen (the sum of ammonium, nitrite, and nitrate) consumption rate that was determined by linear regression of total nitrogen concentrations obtained from the batch assays. The control group was set without the addition of Fe_3O_4 particles.

5.3. Determination of intracellular and extracellular substrate concentrations

AnGS (1.0 g, wet) was collected and transferred into a serum bottle, along with medium solution of 45 mL (Table. S1). Afterwards, 5 mL of Fe_3O_4 particles stock suspensions (2.0 g Fe_3O_4/L) were added into the medium, achieving a concentration of ~200 mg Fe_3O_4/L. After that, 0.125 mL ammonium stock solution ($(NH_4)_2SO_4$ of 20.0 g-N/L) and 0.125 mL of nitrite stock solution ($NaNO_2$ of 24.0 g-N/L) were added to the bottle to elevate the initial ammonium and nitrite concentrations to ~50 and ~60 mg-N/L, respectively. The mixed liquid was mixed in a shaker at a speed of 180 rpm at 35 °C. A liquid sample of 1.0 mL was collected after cultivation for 20 mins and 40 mins, respectively, for the determination of the extracellular ammonium and nitrite concentrations. AnGS of 0.2 g was collected to determine the intracellular ammonium and nitrite concentrations. In detail, the collected AnGS was broken and crushed by a glass grinder and subsequently treated by an ultrasonic cleaning machine (KUDOS, Shanghai) with the ultrasonic power at 0.1 W/cm^2 for 2 mins. After that, the solution was centrifuged at 8000 g for 10 mins to remove the supernatant and resuspended to 0.9% NaCl solution to obtain the bacterial suspension. Afterwards, the bacterial suspension was washed with 0.9% NaCl solution three times and then passed through a high-pressure (60 MPa) homogenizer. The ammonium and nitrite in the cell-free extracts were solubilized through adding an 0.1 M HCl stock solution. Following this, the cell-free extracts were centrifuged at 8000 g for 5 mins. Finally, the ammonium and nitrite concentrations in the supernatant were determined and calculated (Tan et al., 2022). The control group was set without the Fe_3O_4 particles dose. Each test was performed in triplicate.

5.4. Determination of anammox granular permeability

Fluorescent microbeads (Thermo Fisher, USA) tracer experiments were applied to evaluate the permeability mass transfer of AnGS (Billings et al., 2015). The spatial distribution of fluorescent microbeads with the diameter of 1 μm (F8851) in AnGS with/without the dosing of Fe_3O_4 particles was investigated. In detail, 1.0 g wet AnGS was transferred into a 50 mL centrifuge tube and then washed three times with 0.9% NaCl solution. After that, the clean AnGS was mixed with 18 mL 0.9% NaCl solution, 2 mL Fe_3O_4 particles stock suspensions and 50 μL fluorescent microbeads dye that was diluted by 10 times. After cultivated for 5 mins in a shaker at a speed of 180 rpm at room temperature (25 °C), the AnGS with the same size was collected and washed three times with 0.9% NaCl solution in the dark. After that, the AnGS was cryo-sectioned into slices with a thickness of 20 μm by a freezing microtome (SHARDON ORYTOME FE, USA). In doing so, the slices were observed, and the intensity of microbeads was detected by a laser scanning confocal microscopy (LSM780, Zeiss, Germany) under the excitation/emission wavelength of 580/605 nm. The Γ value of AnGS was determined using settling experiments. The fluid can pass through the granules when Γ is greater than 1, which indicates the AnGS has the permeability. While it cannot pass through the granules when Γ is less than 1. The detailed process was shown in Text. S1.

5.5. RNA extraction and meta-transcriptomics analysis

During the batch test, the AnGS was collected at 2 h and 4 h, respectively, for the meta-transcriptomics analysis. Total RNAs of biomass samples were extracted using the PNeasy PowerBiofilm Kit

(Qiagen, Dusseldorf, German). The RNA concentrations and purity were then quantified with NanoDrop2000 (Thermo Fisher Scientific, U.S.). After that, rRNA of total RNAs was removed using the Ribo-zero Magnetic kit (Epicentre, an Illumina® company). cDNA libraries were constructed using a TruSeq™ RNA sample prep kit (Illumina, U.S.). The barcoded libraries were paired-end sequenced on the Illumina Hiseq 2500 platform at Majorbio Bio-Pharm Technology Co., Ltd. (Shanghai, China), using the HiSeq 4000 PE Cluster Kit and HiSeq 4000 SBS Kits. All raw Illumina sequence data were submitted to the NCBI under accession number of PRJNA1114917. The detailed meta-transcriptomics analysis was described in Text. S2.

5.6. Chemical analysis

The ammonium, nitrite, nitrate, and VSS concentrations were examined according to the standard methods (APAH, 2017). The intracellular iron contents were determined by the inductively coupled plasma-mass spectrometry (ICP-MS, PerkinElmer Optima 7300 DV, USA) (Jiang et al., 2020). In detail, the sampled AnGS was broken and crushed by a glass grinder and the crushed AnGS was then treated by an ultrasonic cleaning machine (KUDOS, Shanghai) with the ultrasonic power at 0.1 W/cm^2 for 2 mins. After that, the solution was centrifuged at 8000 g for 10 mins to remove the supernatant and resuspended to obtain the bacterial suspension. Afterwards, the intracellular iron content was determined after the mixed-acid digestion (Zhang et al., 2017a). The heme *c* content of AnGS was determined according to the procedures reported in literature (Kang et al., 2020).

5.7. Statistical analysis

The error bars in this study represented the standard deviation from the three biological replicates. The statistical significance of the data between multiple groups was determined with one-way analysis of variance. The different letters between groups considered statistically significant ($p < 0.05$). The SPSS 22.0 software was employed for all statistical analysis.

Supporting Information

E-supplementary data of this work can be found in online version of the paper.

CRediT authorship contribution statement

Dongdong Xu: Writing – original draft, Methodology, Formal analysis, Data curation, Conceptualization. **Aqiang Ding:** Writing – review & editing. **Yang Yu:** Methodology, Data curation. **Ping Zheng:** Supervision. **Meng Zhang:** Supervision. **Zhetai Hu:** Writing – review & editing, Writing – original draft, Conceptualization.

Declaration of competing interest

The authors declare that they have no known competing financial interests or personal relationships that could have appeared to influence the work reported in this paper.

Data availability

Data will be made available on request.

Acknowledgement

This work was financially supported by the National Key Research and Development Program of China (2022YFC3203003), Key Project of the Natural Science Foundation of Zhejiang Province (LZ23E080004), and Fundamental Research Funds for the Central Universities (226-2024-00010).

Supplementary materials

Supplementary material associated with this article can be found, in the online version, at doi:10.1016/j.wroa.2024.100260.

References

APHA, 2017. Standard Methods for the Examination of Water and Wastewater, 23rd ed. American public health association, Washington DC.
Billings, N., Birjiniuk, A., Samad, T.S., Doyle, P.S., Ribbeck, K., 2015. Material properties of biofilms-a review of methods for understanding permeability and mechanics. Rep. Prog. Phys. 78 (3), 36601.
Bagchi, S., Lamendella, R., Strutt, S., Van Loosdrecht, M.C.M., Saikaly, P.E., 2016. Metatranscriptomics reveals the molecular mechanism of large granule formation in granular anammox reactor. Sci. Rep. 6 (1), 28327.
Chen, H., Zhang, B., Yu, C., Zhang, Z., Yao, J., Jin, R., 2021. The effects of magnetite on anammox performance: phenomena to mechanisms. Bioresour. Technol. 337, 125470.
Dai, B., Yang, Y., Wang, Z., Wang, J., Yang, L., Cai, X., Wang, Z., Xia, S., 2023. Enhancement and mechanisms of iron-assisted anammox process. Sci. Total Environ. 858, 159931.
Dong, Z., Yu, M., Cai, Y., Ma, Y., Chen, Y., Hu, B., 2023. Directed regulation of anammox communities based on exogenous siderophores for highly efficient nitrogen removal. Water. Res. 243, 120394.
Ferousi, C., Lindhoud, S., Baymann, F., Kartal, B., Jetten, M., Reimann, Joachim., 2017. Iron assimilation and utilization in anaerobic ammonium oxidizing bacteria. Curr. Opin. Chem. Biol. 37, 129–136.
Feng, F., Liu, Z., Tang, X., Wu, X., Qu, C., How, S.W., Wu, D., Xiao, R., Tang, C., Lin, Z., Chai, L., Chen, G., 2023. Dosing with pyrite significantly increases anammox performance: its role in the electron transfer enhancement and the functions of the Fe-N-S cycle. Water. Res. 229, 119393.
Fu, R., Hu, X., Zhang, H., Yan, Y., Zhou, W., Wang, J., 2021. Investigation of the influence of Fe_3O_4-water nanofluids on capillary performance in microgrooves wick. Appl. Therm. Eng. 182, 115899.
Hou, X., Liu, S., Zhang, Z., 2015. Role of extracellular polymeric substance in determining the high aggregation ability of anammox sludge. Water. Res. 75, 51–62.
Jin, R., Yang, G., Yu, J., Zheng, P., 2012. The inhibition of the Anammox process: a review. Chem. Eng. J. 197, 67–79.
Jiang, M., Feng, L., Zheng, X., Chen, Y., 2020. Bio-denitrification performance enhanced by graphene-facilitated iron acquisition. Water. Res. 180, 115916.
Kartal, B., Kuenen, J.G., van Loosdrecht, M.C., 2010. Sewage treatment with anammox. Science (1979) 328 (5979), 702–703.
Kang, D., Li, Y., Xu, D., Li, W., Li, W., Ding, A., Wang, R., Zheng, P., 2020. Deciphering correlation between chromaticity and activity of anammox sludge. Water. Res. 185, 116184.
Lotti, T., Kleerebezem, R., Abelleira-Pereira, J.M., Abbas, B., van Loosdrecht, M.C.M., 2015. Faster through training: the anammox case. Water. Res. 81, 261–268.
Li, S., Torsæter, O., Lau, H.C., Hadia, N.J., Stubbs, L.P., 2019. The impact of nanoparticle adsorption on transport and wettability alteration in water-wet berea sandstone: an experimental study. front. Physics. (College Park. Md) 7, 74.
Mu, Y., Yu, H., Wang, G., 2006. Permeabilities of anaerobic CH_4-producing granules. Water. Res. 40 (9), 1811–1815.
Ma, H., Zhang, Y., Xue, Y., Zhang, Y., Li, Y.Y., 2019. Relationship of heme c, nitrogen loading capacity and temperature in anammox reactor. Sci. Total Environ. 659, 568–577.
Peng, M., Yu, X., Guan, Y., Liu, P., Yan, P., Fang, F., Guo, J., Chen, Y., 2019. Underlying promotion mechanism of high concentration of silver nanoparticles on anammox process. ACS. Nano 13 (12), 14500–14510.
Strous, M., Kuenen, J.G., Jetten, M.S.M., 1999. Key physiology of anaerobic ammonium oxidation. Appl. Environ. Microbiol. 65, 3248–3250.
Shi, Z., Guo, Q., Xu, Y., Wu, D., Liao, S., Zhang, F., Zhang, Z., Jin, R., 2017. Mass transfer characteristics, rheological behavior and fractal dimension of anammox granules: the roles of upflow velocity and temperature. Bioresour. Technol. 244, 117–124.
Su, Z., Liu, T., Guo, J., Zheng, M., 2023. Nitrite oxidation in wastewater treatment: microbial adaptation and suppression challenges. Environ. Sci. Technol. 57 (34), 12557–12570.
Tang, C., Zheng, P., Wang, C., Mahmood, Q., Zhang, J., Chen, X., Zhang, L., Chen, J., 2011. Performance of high-loaded ANAMMOX UASB reactors containing granular sludge. Water. Res. 45 (1), 135–144.
Tang, C., Duan, C., Yu, C., Song, Y., Chai, L., Xiao, R., Wei, Z., Min, X., 2017. Removal of nitrogen from wastewaters by anaerobic ammonium oxidation (ANAMMOX) using granules in upflow reactors. Environ. Chem. Lett. 15 (2), 311–328.
Tan, X., Nie, W., Xie, G., Dang, C., Wang, X., Xing, D., Liu, B., Ding, J., Ren, N., 2022. Deciphering the inhibition of ethane on anaerobic ammonium oxidation. Environ. Sci. Technol. 56 (18), 13419–13427.
van der Star, W.R.L., Abma, W.R., Blommers, D., Mulder, J., Tokutomi, T., Strous, M., Picioreanu, C., van Loosdrecht, M.C.M., 2007. Startup of reactors for anoxic ammonium oxidation: experiences from the first full-scale anammox reactor in Rotterdam. Water. Res. 41 (18), 4149–4163.

Wang, Y., Ma, X., Zhou, S., Lin, X., Ma, B., Park, H., Yan, Y., 2016. Expression of the *nirS*, *hzsA*, and *hdh* genes in response to nitrite shock and recovery in *candidatus* kuenenia stuttgartiensis. Environ. Sci. Technol. 50 (13), 6940–6947.
Wang, H., Fan, Y., Zhou, M., Wang, W., Li, X., Wang, Y., 2022. Function of Fe(III)-minerals in the enhancement of anammox performance exploiting integrated network and metagenomics analyses. Water. Res. 210, 117998.
Wang, W., Wang, Y., 2023. Determining the mechanism for biomass segregation between granules and flocs in anammox granular system from the prospective of EPS. Chem. Eng. J. 475, 146028.
Weng, X., Fu, H., Mao, Z., Yan, P., Xu, X., Shen, Y., Chen, Y., 2023. Fate of iron nanoparticles in anammox system: dissolution, migration and transformation. J. Environ. Manage. 348, 119323.
Xu, J.J., Cheng, Y.F., Jin, R.C., 2020. Long-term effects of Fe_3O_4 NPs on the granule-based anaerobic ammonium oxidation process: performance, sludge characteristics and microbial community. J. Hazard. Mater. 398, 122965.
Xu, D., Fan, J., Li, W., Chen, W., Pan, C., Kang, D., Li, Y., Shan, S., Zheng, P., 2021a. Deciphering correlation between permeability and size of anammox granule: "pores as medium". Water Res. 191, 116832.
Xu, D., Fan, J., Pan, C., Kang, D., Li, W., Chen, W., Zhang, M., Hu, B., Zheng, P., 2021b. Dimension effect of anammox granule: potential vs performance. Sci. Total Environ. 795, 148681.
Yu, H., He, Y., Li, P., Li, S., Zhang, T., Rodriguez-Pin, E., Du, S., Wang, C., Cheng, S., Bielawski, C.W., Bryant, S.L., Huh, C., 2015. Flow enhancement of water-based nanoparticle dispersion through microscale sedimentary rocks. Sci. Rep. 5 (1), 8702.
Zhang, Z., Xu, J., Shi, Z., Cheng, Y., Ji, Z., Deng, R., Jin, R., 2017a. Combined impacts of nanoparticles on anammox granules and the roles of EDTA and S^{2-} in attenuation. J. Hazard. Mater. 334, 49–58.
Zhang, Z., Xu, J., Shi, Z., Cheng, Y., Ji, Z., Deng, R., Jin, R., 2017b. Short-term impacts of Cu, CuO, ZnO and Ag nanoparticles (NPs) on anammox sludge: cuNPs make a difference. Bioresour. Technol. 235, 281–291.
Zhao, J., Zhang, B., Zuo, J., 2019. Response of anammox granules to ZnO nanoparticles at ambient temperature. Environ. Technol. Innov. 13, 146–152.
Zheng, M., Hu, Z., Liu, T., Sperandio, M., Volcke, E.I.P., Wang, Z., Hao, X., Duan, H., Vlaeminck, S.E., Xu, K., Zuo, Z., Guo, J., Huang, X., Daigger, G.T., Verstraete, W., van Loosdrecht, M.C.M., Yuan, Z., 2024. Pathways to advanced resource recovery from sewage. Nat. Sustain.